

AUTOSLIDE: AUTOMATIC STROKE LESION IDENTIFICATION

A Project Report

submitted by

A SHRIKANT

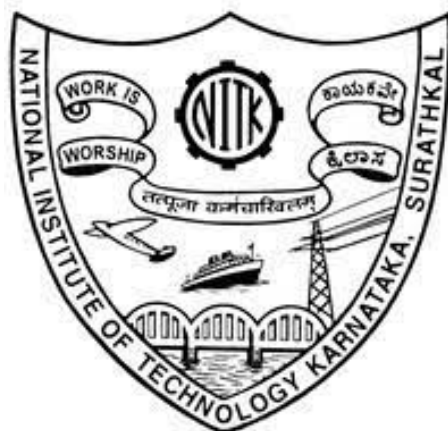
DIPANSHU BARNWAL

*in partial fulfilment of the requirements
for the award of the degree of*

BACHELOR OF TECHNOLOGY

Under the supervision of

Dr. Deepu Vijayasenan



DEPARTMENT OF ELECTRONICS & COMMUNICATION ENGINEERING

NATIONAL INSTITUTE OF TECHNOLOGY KARNATAKA, SURATHKAL

CERTIFICATE

This is to certify that the B.Tech Project Work Report entitled **AutoSLIDE: Automatic Stroke Lesion Identification** submitted by:

- **181EC101 A Shrikant**
- **181EC212 Dipanshu Barnwal**

as the record of the work carried out by them, is accepted as *the B.Tech Project Work Report* submission in partial fulfillment of the requirements for the award of degree of **Bachelor of Technology in Electronics and Communication Engineering** in the Department of Electronics and Communication Engineering at National Institute of Technology Karnataka, Surathkal during the academic year 2021-2022.

Project Guide

Dr. Deepu Vijayasenan
Associate Professor
Dept. of E & C Engineering
NITK, Surathkal

Chairman - DUGC

DECLARATION

by the B.Tech students

We hereby *declare* that the Project Work Report entitled **AutoSLIDE: Automatic Stroke Lesion Identification** which is being submitted to the **National Institute of Technology Karnataka, Surathkal** for the award of the Degree of Bachelor of Technology in Electronics and Communication Engineering is a *bonafide report of the research work carried out by us*. The material contained in this Project Work Report has not been submitted to any University or Institution for the award of any degree.

181EC101 A Shrikant

181EC212 Dipanshu Barnwal

Department of Electronics and Communication Engineering

Place: NITK, Surathkal

Date: December 10, 2021

Acknowledgement

We are indebted to our guide, Dr. Deepu Vijayasenan, Associate Professor, National Institute of Technology Karnataka, Surathkal, for mentoring us throughout our project work. We would also like to thank Dr. Vikram Shenoy Handiru, Associate Research Scientist at Kessler Foundation, for providing us this opportunity to work on this project and his continued guidance as mentor throughout the project. Their constant encouragement and technical insights were invaluable throughout the duration of the project.

Finally, we would like to thank our parents, friends and colleagues for their constant support and motivation.

Abstract

Stroke is one of the leading causes of deaths among the world population and automatic identification of stroke lesions can be of major advantage for radiologists to confirm their presence. In this project, we aimed to automate the process of stroke lesion segmentation using deep Convolutional Neural Networks (CNNs) by analyzing the performance of two architectures, namely, 3D Res-UNET and 3D MI-UNET. 3D Res-UNET incorporates skip connections to alleviate the gradient vanishing problem while training. 3D MI-UNET on the other hand, takes the brain parcellations into account, which includes White Matter (WM), Grey Matter (GM) and Cerebrospinal Fluid (CSF). The inclusion of WM, GM and CSF along with the raw MRI volumes increases the robustness of the model and provides better segmentation results.

The results show that the 3D MI-UNET architecture outperforms the 3D Res-UNET architecture by a dice score of about 2% and Haussdorff distance of about 2 voxels. We expect to improve these results by studying various algorithms like adversarial learning, subpixel information etc. to improve the performance of the model. We also aim to include these implementation to the framework for computing automatic stroke lesions.

Contents

Certificate	i
Declaration	ii
Acknowledgement	iii
Abstract	iv
1 Introduction	1
2 Related Work	2
3 Methodology	3
3.1 ATLAS Dataset	3
3.2 3D UNET	3
3.3 3D Res-UNET	4
3.4 Brain Parcellation and 3D MI-UNET	5
4 Implementation	7
4.1 Dataset and Training Setup	7
4.2 Evaluation	9
4.3 Implementation Code	9
5 Results and Inferences	10
Conclusion and Future Work	12
Bibliography	13
Appendix	16

Section 1

Introduction

Stroke is one of the leading causes of death, especially in the United States. Recent studies reveal every 40 seconds, a person experience a stroke, which ends up having the disabilities such as paralysis and mental disorders over a long term [1]. Stroke is a cerebrovascular disease which occurs due to the blockage of blood supply in the brain and may injure the nervous system later. Rehabilitation is needed for the stroke recovery, but it does require specialized treatments as it varies from person to person [2]. The identification of stroke lesions prove to be beneficial for rehabilitation. T1-weighted (T1W) magnetic resonance imaging (MRI) is the most commonly used to study the structural and functional changes in the brain. Automated tracing of the lesions can be very useful as evaluations by experts are costly and time consuming.

However, the task of automatic segmentation of lesions from T1W MRI volumes is quite challenging. This is due to the nature of 3D stroke lesions whose location and shape vary, with the volumes ranging from tens to millions of cubic millimeters. The deep learning has gained significant popularity and attention in radiology imaging due to its promising results and high prediction rate. There are several approaches in the deep learning paradigm, which can be used for effective and fast computation.

Recently, convolutional neural networks (CNNs) have achieved robust performance in various image analysis tasks, where 3D CNNs can extract 3D spatial features. Since diagnosing stroke lesions by radiologists requires analysis of a lesion and its surrounding area, 3D CNNs are suitable for this task and hence generalize the contextual information of voxels (i.e., volumetric pixels) into analysis by capturing both low-level local features (i.e., edges and corners) and high-level global features (i.e., the anatomy of brains).

In this project we aim to explore two of the state-of-the-art models for lesion segmentation, namely, 3D Res-UNET (Residual UNET) and 3D MI-UNET (Multi-Inputs UNET). These architectures differ mainly in the number of input volumes for an example data point considered.

Section 2

Related Work

After the advancement of CNNs in generalizing spatial features, there have been several attempts by various researchers to incorporate CNNs for the semantic segmentation tasks. In most of the 2D CNN methods, a 3D volume is sliced along one dimension to give a set of 2D images and the stroke lesion is independently predicted for each slice. To capture long-range dependencies, Qi et al. proposed XNet using depth-wise separable convolution and non-local blocks [3] and reported an average Dice of 48.67% on the anatomical tracing of lesions after stroke (ATLAS) dataset [4]. Yang et al. proposed a cross-level fusion and context inference network (CLCI-Net) [5], making use of features at different scales to discriminate fine structures with similar intensity profiles and achieved an average Dice of 48.1% on a subset of the ATLAS dataset. Researchers have however found that in such segmentation procedures, the 3D context information in MR image is ignored, and hence the predicted segmentation will have no inter-slice smoothness.

So the necessity for incorporating volumetric convolutions and 3D CNNs for the volumetric segmentation problems was widely addressed. Zhang et al. proposed a deep 3D CNN equipped with dense connectivity to segment stroke lesions from diffusion-weighted MR image and achieved an average Dice of 58% on the ISLES 2015 dataset [6]. Zhou et al. put forward a dimension-fusion-UNet (D-UNet) [7] by combining 2D and 3D convolutions at the encoding stage. They achieved an average Dice of 53.49% on a subset of the ATLAS dataset.

Section 3

Methodology

3.1 ATLAS Dataset

ATLAS [4] is a publicly available dataset consisting of T1-weighted MRI volumes of 229 subjects. The entire dataset contains 543 raw nifti files (.nii) and each of those 543 raw files were provided with 1-5 manually annotated stroke lesions. There were primary smoothed lesion masks saved as .voi files as well as additional lesions saved as smooth/raw nifti files. Each volume mask was tested for inter-reliability and intra-reliability using their corresponding F1-scores. The files consisted of volumes of varying dimensions, but on an average contained $180 \times 180 \times 180$ voxel volumes. The size of the stroke lesions in these volumes ranges from 10 mm^3 to $2.8 \times 10^5 \text{ mm}^3$. A T1-weighted MRI volume of the dataset is shown in Figure 3.1.

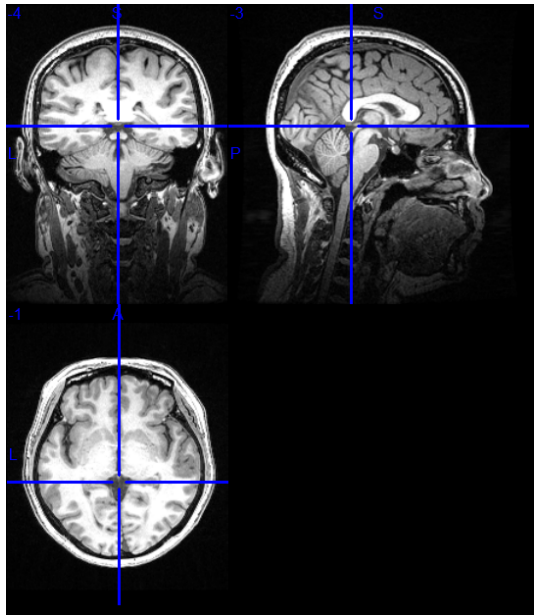


Figure 3.1: ATLAS Dataset [4]: T1-weighted volume

3.2 3D UNET

Our approach towards this lesion identification problem was employing the 3D UNET architecture [8] for semantic segmentation. UNET architecture consists of an encoder (downsampling

CNN network) and a decoder (upsampling CNN network). The encoder extracts image-level features from the input images at different scales, finally reaching a latent space representation. The decoder uses these latent space features as well as features from intermediate scales and reconstructs a semantic segmentation map. The downsampling and upsampling of the feature tensors are achieved by max-pooling and transposed convolutions respectively.

As shown in the Figure 3.2, the gray arrows (left to right) indicates the concatenation operation, where the current outputs are concatenated with previous outputs of same scale, and thus used in further convolutions.

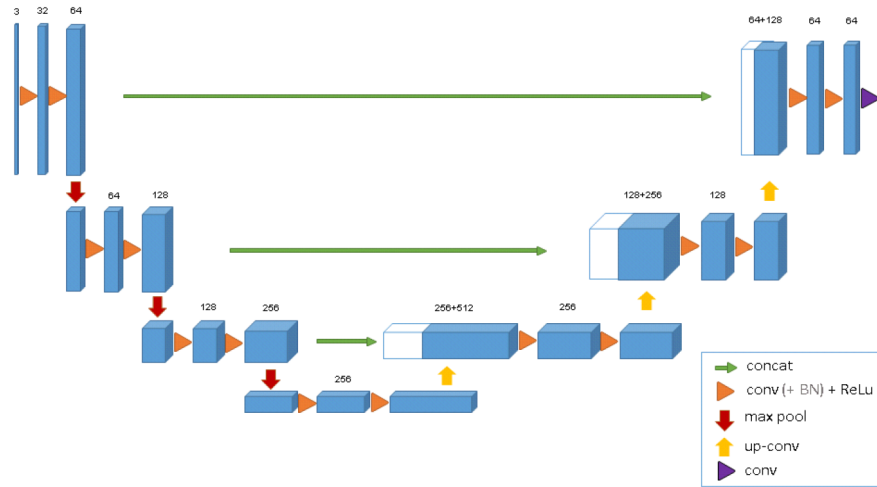


Figure 3.2: 3D UNET Architecture [9]

3.3 3D Res-UNET

3D Res-UNET is one of the variants of the UNET architecture that is explored in this work for modelling the semantic segmentation problem [10]. 3D Res-UNET consists of residual connections between the 3D convolutional layers as shown in Figure 3.4. The residual connections are used in the convolution blocks in UNET to overcome the vanishing gradient problem [11]. The convolutional blocks are designed as shown in Figure 3.3a, where ‘ReLU’ refers to the Rectified Linear Unit which serves as an activation function, ‘gn’ refers to group normalization, which is experimented here instead of the traditional batch normalization. The resultant features are padded accordingly to match the feature shape of the skip connected features for element-wise addition.

Group normalization is a normalization layer that splits the channel into a fixed number of groups and normalizes the features within each group [12]. Due to the higher dimension of 3D volumes for training, the batch sizes while training are restricted to a small number. Group normalization ensures a better normalization while training with smaller batch sizes than batch normalization that fails to give robust results for small batch sizes.

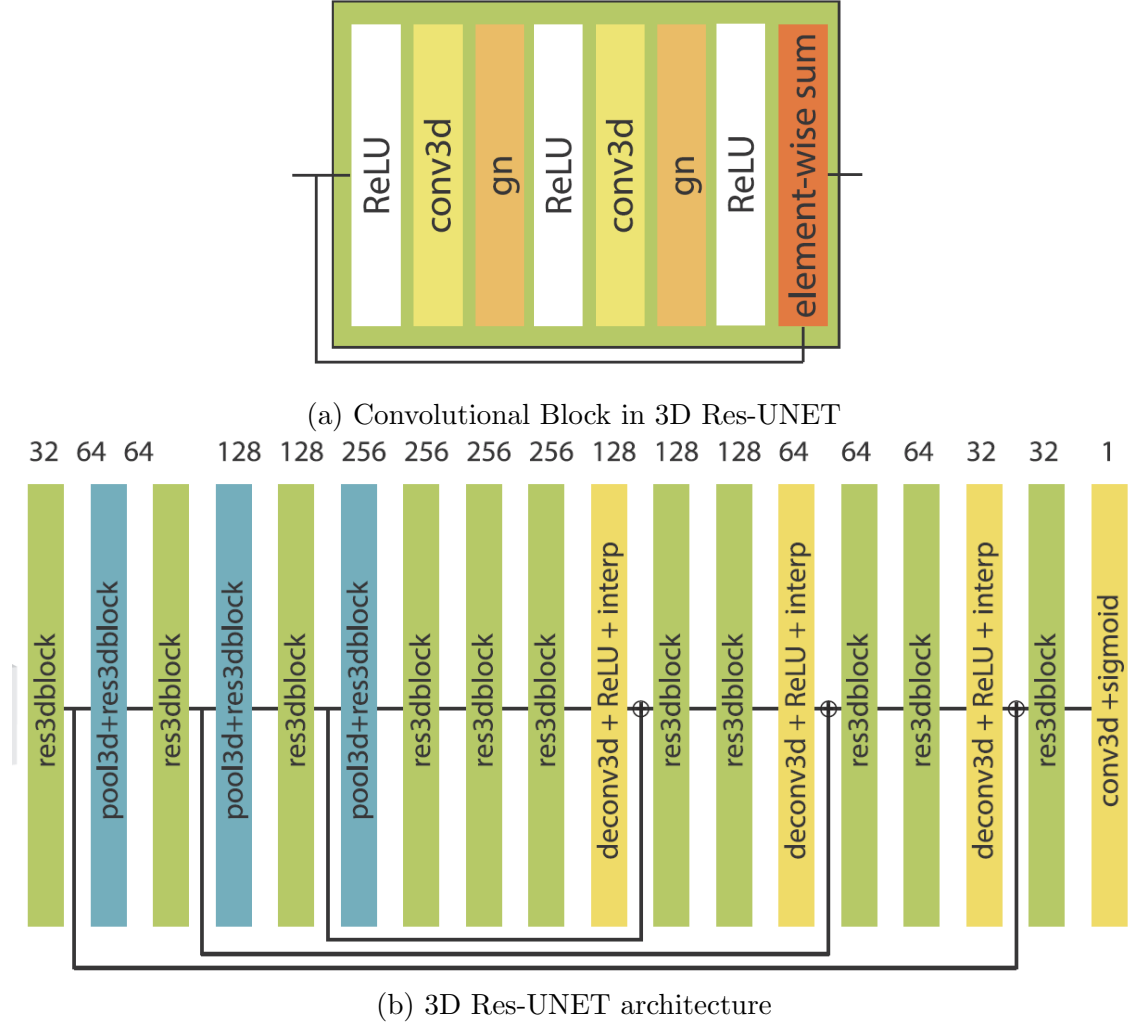


Figure 3.3: Res-UNET Architecture [10]

3.4 Brain Parcellation and 3D MI-UNET

Brain Parcellation refers to segmenting the MRI volumes into White Matter (WM), Gray Matter (GM) and Cerebrospinal Fluid (CSF). According to [13], most of the stroke lesions are located in either the White Matter (WM) or the Gray Matter (GM). Chen et al. showed that stroke occurs at GM since GM has a high cerebral blood flow level due to its high metabolic demand [14]. Wang et al. nevertheless showed that the majority of damages caused by stroke are located in WM because WM has a low blood supply and is more susceptible to ischemia than other brain regions [15]. From these studies, it is clear that the process of locating the stroke lesions can be made more robust if WM and GM volumes are considered while training the neural network.

The MRI volumes are fed to an optimization algorithm called LDDMM (Large Deformation Diffeomorphic Mapping)-image, which uses a template image and the input image to generate the brain parcellations [16]. These result in gray matter (GM) and white matter (WM). Figure 3.4a shows the parcellated result where green pixels corresponds to GM, red corresponds

to WM and blue corresponds to CSF. The algorithm is implemented in MATLAB using the CAT-12 toolbox which generates the parcellations for every MRI volume along with the analysis reports.

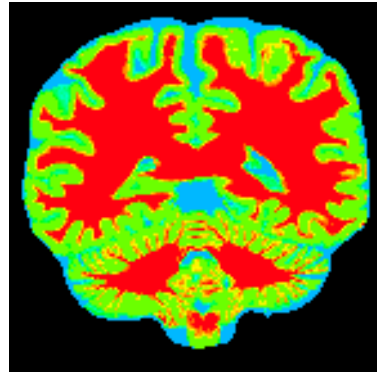
LDDMM (Large Deformation Diffeomorphic Mapping)

The LDDMM-image is a robust optimization algorithm that aims to segment a given volume data (I_1) into a number of segments (labels) using a template image (I_0) and its corresponding template label (L_0) [16]. The volumes I_0, I_1 are both assumed to be real valued functions defined on the space $\Omega \in \mathbb{R}^3$. The aim is to learn a diffeomorphic mapping function $\phi : \Omega \rightarrow \Omega$ such that $I_0 \circ \phi^{-1}$ is aligned to I_1 . The mapping function is solved as a Laplacian-based optimization problem, resulting in a function ϕ^* as an approximation to ϕ .

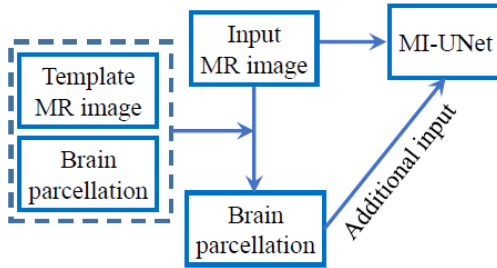
The resulting parcellation label for I_1 is obtained as,

$$L_1 = L_0 \circ (\phi^*)^{-1}$$

The parcellated volumes are fed to the 3D MI-UNET (Multi-Inputs UNET) model for training along with the raw MRI volumes as shown, thus MI-UNET takes multiple inputs for segmenting the stroke lesions, as shown in Figure 3.4b. The parcellated volume and raw MRI volume are concatenated channel-wise and trained to locate the lesions [17].



(a) Parcellated MRI scan



(b) Block Diagram: 3D MI-UNET [17]

Figure 3.4: Multi-Inputs UNET: Brain Parcellation and Block Diagram

Section 4

Implementation

4.1 Dataset and Training Setup

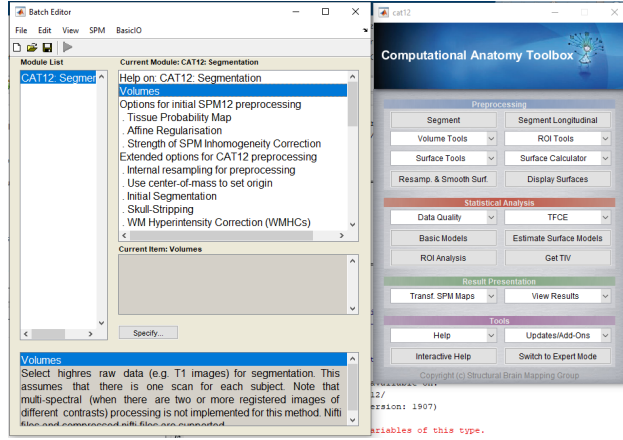
The dataset was split into train, validation and test folds, with the ratio of 75%-15%-10% split resulting in 408 training volumes, 80 validation volumes and 55 test volumes. For training the models, the MRI volumes were cropped with a size of 120x120x120 in random fashion and fed to the network, since the MRI volumes ATLAS dataset were of varying sizes and resizing them into a particular size was found to be not appropriate.

The implementation was done in Python 3.x, using PyTorch as the framework and Google Colab Pro GPU as the computational hardware. Both the networks, 3D ResUNET and 3D MI-UNET were trained using Adam optimizer with a learning rate of 0.0001 and a momentum of 0.9, with weight decay of 1e-4, for 100 epochs. For all layers in the network, the learnable parameters (weights) were initialized with the kaiming-uniform initialization, also known as He-Initialization [18]. For validating our approach during training, we used the centers of lesion masks to crop the volumes with each spatial dimension as 120 from the validation dataset. This ensures that we measure a consistent validation performance. A cosine annealing learning rate scheduler [19] was employed while training the networks.

Brain Parcellation

Brain parcellation was implemented using CAT12 (Computational Anatomy Toolbox) and MATLAB, as shown in Figure 4.1. The toolbox was made open-source by the researchers at Structural Brain Mapping Group (SBMG) at the University of Jena. The toolbox consisted of various functionalities for analyzing T1-weighted MRI volumes, one of which is Voxel-Based Morphometry (VBM) which parcellated the input volumes into WM, GM and CSF. There are various other functionalities like skull stripping, Deformation-based Morphometry (DBM), Spatial Normalization etc.

The entire dataset with 543 volumes was fed as input to the toolbox which resulted in several kinds of output volumes, namely, individual tissues (WM, GM and CSF), followed by a segmentation map with labelled voxel locations of the tissues and some additional variables like noise fraction, absolute tissue volume, tissue thickness etc.



(a) CAT12 Toolbox

Segmentation: D:\Books and files\7th sem\Major Project\images\50.nii

Version: 0.9 / Release: 7 / SPML2 / CAT12 / seg:

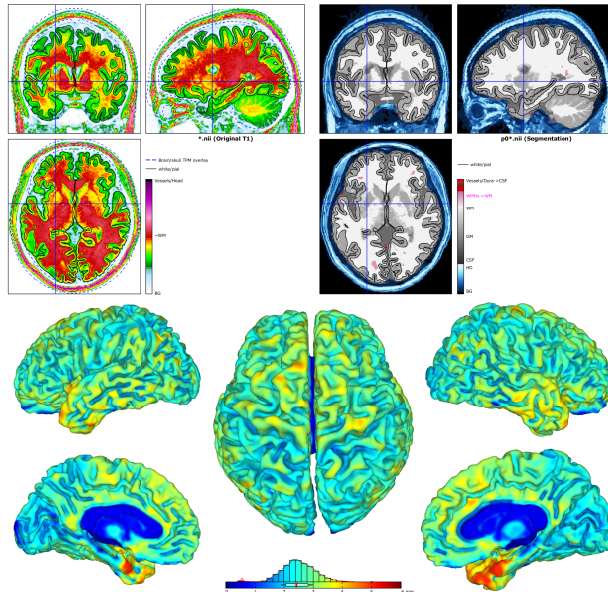
Tissue Probability Map: colorref(pobj1, 0, 0), MATLAB6.5(2008b)\toolbox\spm12\lpm\TPM.nii
 Optimized Shelling Registration to: \v_MNI152NLin2009Asym\Temp\shells_0_GS.nii
 affreg / APP / sCox2:
 blastr:
 LAS strength / Skull Stripping:
 Initial Segmentation / WM Correction / Int. Res.:
 Voxel resolution (original > internal > PBR; vox): 1.00x1.00x1.00 > 1.00x1.00x1.00 > 0.50x mm³, 1.50x mm³

Image and Preprocessing Quality:

Resolution:	85.00% (B)
Noise:	77.96% (C+)
Bias:	93.24% (A-)
Weighted average (QQR):	93.94% (C+)
Mean surface Euler number:	12
Defect area:	0.25%
Processing time:	55:01 min

Volumes:

CSF	GM	WMI	
Absolute volume:	190	603	484 cm ³
Relative volume:	14.9	47.2	37.9 %
TIV:	1276 cm ³		
Thickness:	2.49x0.64 mm		



(b) Parcellation and details

Figure 4.1: Implementing Brain Parcellation with CAT-12

Loss function

The weighted combination of BCE and dice loss is used here to measure the dissimilarity between groundtruth and prediction, where α represents the weight for the dice loss, as shown below.

$$Loss = \alpha \cdot Dice Loss + (1 - \alpha) \cdot BCE$$

$$\text{Dice Loss} = 1 - \frac{2 \sum_{ij} Y_{ij} \cdot \hat{Y}_{ij}}{\sum_{ij} (Y_{ij} + \hat{Y}_{ij})}$$

$$BCE = -\hat{Y}_{ij} \cdot \log(Y_{ij}) - (1 - \hat{Y}_{ij}) \cdot \log(1 - Y_{ij})$$

where ij represent pixel index, Y_{ij} is groundtruth and \hat{Y}_{ij} is prediction.

For 3D ResUNET, α was set at 0.9. α was decreased to 0.5 for training 3D MI-UNET. This is done because 3D MI-UNET has two concatenated volumes as input and binary cross entropy proves to be useful for measuring the error between parcellated volume and the groundtruth, as observed through experimentation.

4.2 Evaluation

Similarity evaluation metrics are used to quantify the similarity between the predicted output of the model and the ground-truth label. The metrics used in this study are as follows.

$$\begin{aligned} \text{Precision} &= \frac{TP}{TP + FP} & \text{Recall} &= \frac{TP}{TP + FN} \\ \text{Dice score} &= \frac{2TP}{2TP + FN + FP} & \text{Jaccard score} &= \frac{TP}{TP + FN + FP} \end{aligned}$$

TP : True Positives, FP : False Positives, FN : False Negatives, TN : True Negatives

Along with the above standard metrics, we measured the performance of our approaches on the test data by using surface distances, which are generally used for 3D objects. The average symmetric surface distance (ASSD) measures the average of all the distances between the surface vertices of predicted and ground truth regions. The Hausdorff distance measures the maximum symmetric surface distance.

$$ASSD = \frac{\sum_{s_G} d(s_G, S(P)) + \sum_{s_P} d(s_P, S(G))}{|S(G)| + |S(P)|}$$

$$\text{Hausdorff distance} = \max \left\{ \sup_{s_G} d(s_G, S(P)), \sup_{s_P} d(s_P, S(G)) \right\}$$

where $S(G)$ is a set of surface vertices of ground truth and $S(P)$ is that of predicted segmentation region. s_G and s_P denote the surface vertices and so, $d(\cdot)$ gives the minimum distance of a vertex from the surface. Here, \sup denotes the supremum.

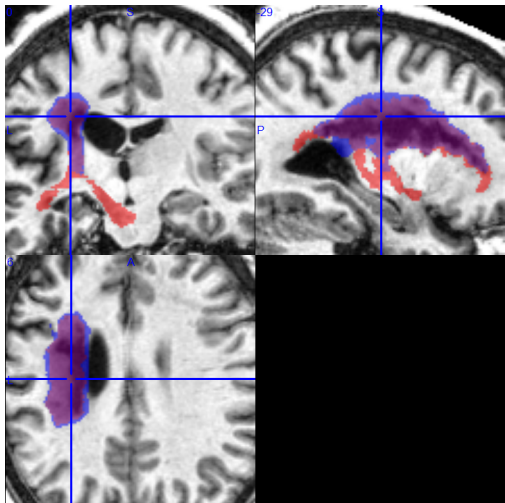
4.3 Implementation Code

The code and trained weights of this study are available [here](#).

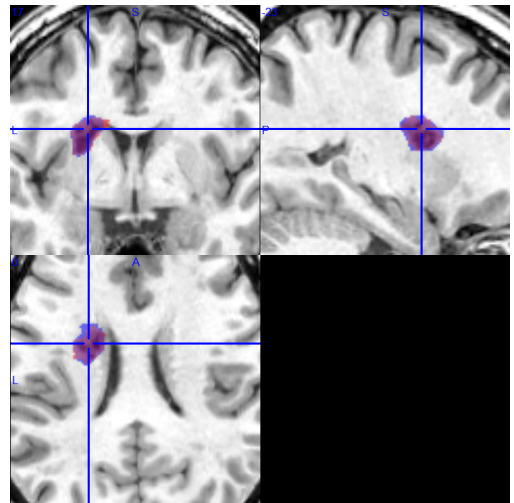
Section 5

Results and Inferences

The segmentation regions of lesions generated from the two methods of 3D Res-UNET and 3D MI-UNET are shown in the Figures 5.1 and 5.2.

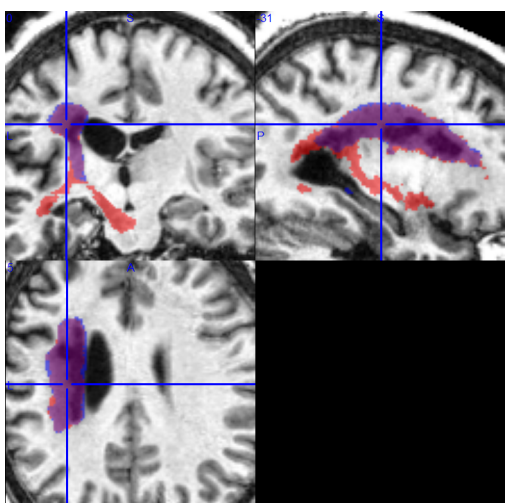


(a) Segmented Lesion 1

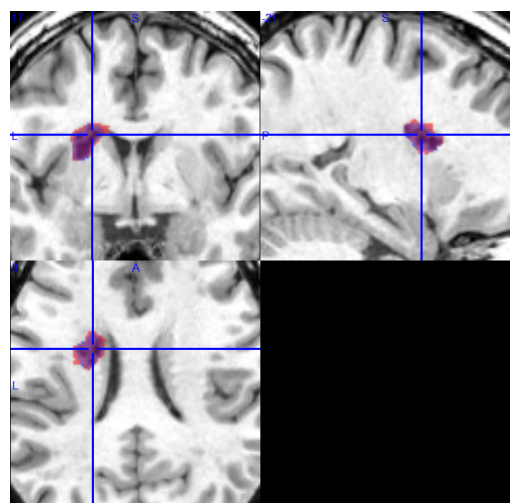


(b) Segmented Lesion 2

Figure 5.1: Segmentation results on 3D Res-UNET. Blue: Predicted Lesion and Red: Ground Truth Lesion



(a) Segmented Lesion 1



(b) Segmented Lesion 2

Figure 5.2: Segmentation results on 3D MI-UNET. Blue: Predicted Lesion and Red: Ground Truth Lesion

The performance of the developed techniques evaluated on the test dataset using the standard performance metrics as well as the surface distances are mentioned in Table 5.1. From the Figures 5.1, 5.2 and Table 5.1, the following inferences can be made.

1. It is observed that the segmentation masks generated from 3D MI-UNET have low false positives and better defined boundaries between foreground and background, than that of Res-UNET. So, the additional input (brain parcellation) in 3D MI-UNET improves the performance in identifying the stroke lesions.
2. Moreover, from Table 5.1, it can be established quantitatively that 3D MI-UNET performs better than 3D Res-UNET by a margin of about 2%.
3. However, both the models face difficulties in locating and segmenting tiny lesions.

Metrics	3D Res-UNET	3D MI-UNET
Precision	0.6854	0.6664
Recall	0.5355	0.5558
Dice score	0.5429	0.5660
Jaccard score	0.4289	0.4638
ASSD	6.1129	5.551
Hausdorff Distance	32.7544	30.8755
Parameters	18,438,561	22,579,137

Table 5.1: Comparison of different Stroke Lesion segmentation results on the test data

Conclusion and Future Work

The results obtained indicate that the 3D MI-UNET, with its additional input clearly provides a better segmentation results as compared to the 3D Res-UNET architecture. Furthermore the results and similarity metrics obtained from these methods match the results of the base paper with a very few number of training iterations. This clearly indicates that there are grounds for improvement in the architecture which can lead to a superior performance as compared to the state-of-the-art approach.

This lays a foundation for our future work which is planned out to include the following,

- Improvise the state-of-the-art algorithm by incorporating prior knowledge in algorithms like adversarial learning, subpixel learning, etc. and modified loss functions (in consultation with the project collaborators from NTU Singapore and/or UPenn).
- Disseminate the findings by sharing fully reproducible codebase on Github (or a similar repository) and contribute to the framework to integrate automated stroke lesion maps and the computational modeling of trans-cranial Direct Current Stimulation (tDCS).

Bibliography

- [1] P. Langhorne, J. Bernhardt, and G. Kwakkel, “Stroke rehabilitation,” *Lancet*, vol. 377, no. 9778, pp. 1693–1702, May 2011.
- [2] S. S. Virani, A. Alonso, E. J. Benjamin, M. S. Bittencourt, C. W. Callaway, A. P. Carson, A. M. Chamberlain, A. R. Chang, S. Cheng, F. N. Delling, L. Djousse, M. S. V. Elkind, J. F. Ferguson, M. Fornage, S. S. Khan, B. M. Kissela, K. L. Knutson, T. W. Kwan, D. T. Lackland, T. T. Lewis, J. H. Lichtman, C. T. Longenecker, M. S. Loop, P. L. Lutsey, S. S. Martin, K. Matsushita, A. E. Moran, M. E. Mussolino, A. M. Perak, W. D. Rosamond, G. A. Roth, U. K. A. Sampson, G. M. Satou, E. B. Schroeder, S. H. Shah, C. M. Shay, N. L. Spartano, A. Stokes, D. L. Tirschwell, L. B. VanWagner, C. W. Tsao, and American Heart Association Council on Epidemiology and Prevention Statistics Committee and Stroke Statistics Subcommittee, “Heart disease and stroke statistics-2020 update: A report from the american heart association,” *Circulation*, vol. 141, no. 9, pp. e139–e596, Jan. 2020.
- [3] K. Qi, H. Yang, C. Li, Z. Liu, M. Wang, Q. Liu, and S. Wang, “X-net: Brain stroke lesion segmentation based on depthwise separable convolution and long-range dependencies,” *Medical Image Computing and Computer Assisted Intervention – MICCAI 2019*, p. 247–255, 2019. [Online]. Available: http://dx.doi.org/10.1007/978-3-030-32248-9_28
- [4] S.-L. Liew, J. M. Anglin, N. W. Banks, M. Sondag, K. L. Ito, H. Kim, J. Chan, J. Ito, C. Jung, N. Khoshab, S. Lefebvre, W. Nakamura, D. Saldana, A. Schmiesing, C. Tran, D. Vo, T. Ard, P. Heydari, B. Kim, L. Aziz-Zadeh, S. C. Cramer, J. Liu, S. Soekadar, J.-E. Nordvik, L. T. Westlye, J. Wang, C. Winstein, C. Yu, L. Ai, B. Koo, R. C. Craddock, M. Milham, M. Lakich, A. Pienta, and A. Stroud, “A large, open source dataset of stroke anatomical brain images and manual lesion segmentations,” *bioRxiv*, 2017. [Online]. Available: <https://www.biorxiv.org/content/early/2017/11/08/179614>
- [5] H. Yang, W. Huang, K. Qi, C. Li, X. Liu, M. Wang, H. Zheng, and S. Wang, “Clci-net: Cross-level fusion and context inference networks for lesion segmentation of chronic stroke,” *Medical Image Computing and Computer Assisted Intervention – MICCAI 2019*, p. 266–274, 2019. [Online]. Available: http://dx.doi.org/10.1007/978-3-030-32248-9_30
- [6] R. Zhang, L. Zhao, W. Lou, J. M. Abrigo, V. C. T. Mok, W. C. W. Chu, D. Wang, and L. Shi, “Automatic segmentation of acute ischemic stroke from dwi using 3-d fully

- convolutional densenets,” *IEEE Transactions on Medical Imaging*, vol. 37, no. 9, pp. 2149–2160, 2018.
- [7] Y. Zhou, W. Huang, P. Dong, Y. Xia, and S. Wang, “D-unet: A dimension-fusion u shape network for chronic stroke lesion segmentation,” *IEEE/ACM Transactions on Computational Biology and Bioinformatics*, vol. 18, pp. 940–950, 2021.
- [8] R. Olaf, F. Philipp, and B. Thomas, “U-net: Convolutional networks for biomedical image segmentation,” vol. 9351, 10 2015, pp. 234–241.
- [9] Çiçek, A. Abdulkadir, S. Lienkamp, T. Brox, and O. Ronneberger, “3d u-net: Learning dense volumetric segmentation from sparse annotation,” 06 2016.
- [10] N. Tomita, S. Jiang, M. E. Maeder, and S. Hassanpour, “Automatic post-stroke lesion segmentation on mr images using 3d residual convolutional neural network,” *NeuroImage: Clinical*, vol. 27, p. 102276, 2020. [Online]. Available: <https://www.sciencedirect.com/science/article/pii/S2213158220301133>
- [11] K. He, X. Zhang, S. Ren, and J. Sun, “Deep residual learning for image recognition,” in *2016 IEEE Conference on Computer Vision and Pattern Recognition (CVPR)*, 2016, pp. 770–778.
- [12] Y. Wu and K. He, “Group normalization,” 2018.
- [13] L.-P. Berner, T.-H. Cho, J. Haesebaert, J. Bouvier, M. Wiart, N. Hjort, I. Klærke Mikkelsen, L. Derex, G. Thomalla, S. Pedraza, L. Østergaard, J.-C. Baron, N. Nighoghossian, and Y. Berthezène, “MRI assessment of ischemic lesion evolution within white and gray matter,” *Cerebrovasc Dis*, vol. 41, no. 5-6, pp. 291–297, Feb. 2016.
- [14] C. Chen, A. Bivard, L. Lin, C. R. Levi, N. J. Spratt, and M. W. Parsons, “Thresholds for infarction vary between gray matter and white matter in acute ischemic stroke: A CT perfusion study,” *J Cereb Blood Flow Metab*, vol. 39, no. 3, pp. 536–546, Nov. 2017.
- [15] Y. Wang, G. Liu, D. Hong, F. Chen, X. Ji, and G. Cao, “White matter injury in ischemic stroke,” *Prog Neurobiol*, vol. 141, pp. 45–60, Apr. 2016.
- [16] J. Wu and X. Tang, “A large deformation diffeomorphic framework for fast brain image registration via parallel computing and optimization,” *Neuroinformatics*, vol. 18, no. 2, pp. 251–266, Apr. 2020.
- [17] Y. Zhang, J. Wu, Y. Liu, Y. Chen, E. X. Wu, and X. Tang, “Mi-unet: Multi-inputs unet incorporating brain parcellation for stroke lesion segmentation from t1-weighted magnetic resonance images,” *IEEE Journal of Biomedical and Health Informatics*, vol. 25, no. 2, pp. 526–535, 2021.

- [18] K. He, X. Zhang, S. Ren, and J. Sun, “Delving deep into rectifiers: Surpassing human-level performance on imagenet classification,” 2015.
- [19] I. Loshchilov and F. Hutter, “Sgdr: Stochastic gradient descent with warm restarts,” 2017.

12/2/21, 10:31 AM

National Institute of Technology Karnataka Mail - Report for Major Project AutoSLIDE



Dipanshu Barnwal. <dipanshu.181ec212@nitk.edu.in>

Report for Major Project AutoSLIDE

2 messages

Dipanshu Barnwal. <dipanshu.181ec212@nitk.edu.in>

Thu, Dec 2, 2021 at 10:05 AM

To: Deepu Vijayasenan <deepuv@nitk.edu.in>

Cc: A Shrikant <ashrikant.181ec101@nitk.edu.in>

Dear Sir

We have made the report for the Major Project: Automatic Stroke Lesion identification. We request your approval as we need to submit it for the Endsem evaluation after the approval.

I have attached the report in the mail.

Sincerely

Dipanshu Barnwal
181EC212

 [Major_Project_AUTOSLIDE.pdf](#)
7593K

Deepu Vijayasenan <deepuv@nitk.edu.in>

Thu, Dec 2, 2021 at 10:28 AM

To: "Dipanshu Barnwal." <dipanshu.181ec212@nitk.edu.in>

Cc: A Shrikant <ashrikant.181ec101@nitk.edu.in>

It is fine.. please go ahead

Deepu

[Quoted text hidden]